

# Mapping Chemical Gradients within and along a Fibrous Structural Tissue, Mussel Byssal Threads\*

Received for publication, August 5, 2005, and in revised form, September 14, 2005 Published, JBC Papers in Press, September 15, 2005, DOI 10.1074/jbc.M508674200

ChengJun Sun<sup>†1</sup> and J. Herbert Waite<sup>‡§</sup>

From the <sup>‡</sup>Molecular, Cellular, and Developmental Biology Department and the <sup>§</sup>Chemistry and Biochemistry Department, University of California Santa Barbara, Santa Barbara, California 93106

The byssal thread of a mussel is an extraorganismic connective tissue that exhibits a striking end-to-end gradient in mechanical properties and thus provides a unique opportunity for studying how gradients are made. Mfp-1 (*Mytilus* foot protein-1) is a conspicuous component of the protective outer cuticle of byssal threads given its high 3,4-dihydroxyphenylalanine (Dopa) content at 10–15 mol %. Amino acid analysis of mfp-1 extracted from successive foot sections of *Mytilus galloprovincialis* reveals a post-translationally mediated gradient with highest Dopa levels present in mfp-1 from the accessory gland near the tip of the foot decreasing gradually toward the base. The Dopa content of successive segments of byssal threads decreases from the distal to the proximal end and thus reflects the trend of mfp-1 in the foot. Inductively coupled plasma analysis indicates that certain metal ions including iron follow the trend in Dopa along the thread. Energy-dispersive x-ray spectrometry showed that iron, when present, was concentrated in the cuticle of the threads but sparse in the core. The axial iron gradient appears most closely correlated with the Dopa gradient. The direct incubation of mussels and byssal threads in Fe<sup>3+</sup> supplemented seawater showed that byssal threads are unable to sequester iron from the seawater. Instead, particulate/soluble iron is actively taken up by mussels during filter feeding and incorporated into byssal threads during their secretion. Our results suggest that mussels may exploit the interplay between Dopa and metals to tailor the different parts of threads for specific mechanical properties.

Organisms build a variety of load-bearing materials with unique mechanical properties chiefly by adjusting two parameters, composition and architecture. In principle, composition and architecture in tissues can be adjusted either abruptly or gradually, but it is becoming increasingly evident that nature prefers gradients (1, 2). Manufactured materials with graded mechanical properties show superior resistance to contact deformation and damage (2), and this would also have adaptive benefits in nature, but there are few studies of how natural gradients are made. Recent results with byssal threads are revealing how composition and microstructural gradients are combined into a functional material.

Byssal threads in mussels (*Mytilus* sp.) collectively serve as a robust holdfast for attachment to hard substrates in the turbulent intertidal zone. In the case of *Mytilus edulis*, a typical byssus consists of 40–100

threads each ~4–5-cm long (3). Each thread is rapidly manufactured by the foot of the mussel via an injection-molding-like process and becomes part of an extensive extraorganismic, extracellular connective tissue that enables strong substrate attachment for mussels in the intertidal zone (3). In turbulent flow, suspended sand commonly abrades all exposed parts of mussels, and organic structures such as the periostracum are particularly prone to wear. The wear of byssal threads has not been specifically examined, although the ultrastructure of a protective outer cuticle has been noted (4, 5).

Earlier studies have demonstrated that the thread core consists of an axially graded material in both mechanical and molecular properties. Three collagenous proteins, preCOL<sup>2</sup>-P, -D, and -NG make up the bulk of the thread core with two of these, D and P, providing the building blocks for molecular gradients (6). The preCOLs are bent-core or banana-shaped structures because of the kinks in collagen triple helix (7). The mechanical consequences of the molecular gradients presumably arise from the flanking domains of preCOLs D and P, which resemble dragline silk and elastin, respectively (1). The core region of the thread is coated with a 4–5- $\mu$ m thick layer of protective cuticle (thicker at the proximal end of thread), of which mfp-1 is a major component (3, 8). It is intriguing to materials research how this cuticle both protects the core and accommodates the strain of nearly 70% exhibited by the thread core (9, 10)

Mfp-1 purified from *M. edulis* (mfp-1) has 85 decapeptide and hexapeptide repeat sequences with the decapeptide, AKPSYP\*PTYK, being the most abundant one in which P stands for hydroxyproline, P\* stands for dihydroxyproline, and Y stands for 3,4-dihydroxyphenylalanine (Dopa), (11, 12). It has a mass of ~110 kDa and contains an average of 10–15 mol % Dopa (13). Mfp-1 from *Mytilus galloprovincialis* (Mfp-1) has not been characterized; however, its sequence has been deduced from cDNA to share a 78% identity with mfp-1 without the hexapeptide repeats (14). Besides being a structural component of the thread cuticle, mfp-1 has been used as a universal cell and tissue attachment factor, and the Dopa moiety is being developed as a biomimetic tether to attach polyethylene glycol to biomedical implant surfaces (15, 16). Interest in Dopa initially came from its tendency to oxidize and cross-link in the process known as quinone tanning (17). In the presence of metal ions such as Fe(III), Dopa can form catechol complexes with exceptional stability (18). Dopa-containing proteins produced by certain marine invertebrates are believed to function in adhesion, sclerotization, and wound repair (18). The function of mfp-1 in byssal thread cuticle is not known yet. It is believed that mfp-1 (from *M. edulis*) is deposited as a cuticular varnish layer over the entire thread (8). Because of the extensive cross-linking of mfp-1 in the threads, there have been few reliable data on the localization and distribution of mfp-1 in the thread.

\* This research was supported by Grant R01 DE015415 from the National Institutes of Health and Grant NCC-1-02037 NASA University Research, Engineering and Technology Institute in Bio-Inspired Materials. The costs of publication of this article were defrayed in part by the payment of page charges. This article must therefore be hereby marked "advertisement" in accordance with 18 U.S.C. Section 1734 solely to indicate this fact.

<sup>†</sup> To whom correspondence should be addressed: MCD Biology Dept., University of California, Santa Barbara, CA 93106. Tel.: 805-893-5787; Fax: 805-893-7998; E-mail: sun@lifesci.ucsb.edu.

<sup>2</sup> The abbreviation used are: preCOL, precollagen; Dopa, 3,4-dihydroxyphenylalanine; NBT, nitro blue tetrazolium; EDS, energy dispersive spectrometry; ICP, inductively coupled plasma.

Iron and other metals are known to be associated with byssal threads (19–21). George *et al.* (22) first demonstrated using  $^{59}\text{Fe}$  that instead of being directly adsorbed from sea water into the thread, the iron was first filtered from seawater and then transported by amoebocytes to various tissues of the mussel particularly the byssal threads. To date, the function of metals in byssus is still debated. Taylor *et al.* (13, 18) showed that mfp-1 and Dopa-containing peptides derived from mfp-1 bind iron(III) *in vitro* to form ferric catecholate complexes with a  $\log K_s$  higher than 38. Stability constants of comparable magnitude are also known for catecholate complexes with Al(III) and Si(IV) (16). Mfp-1 and  $\text{Fe}^{3+}$  combine to form cross-links through the Dopa moiety (23, 24). Dopa groups have been shown to have a strong interaction with  $\text{TiO}_2$  surfaces (16). Unfortunately, how the metals react with proteins in the thread remains unknown. Information on this will greatly help to understand the structure and function of the byssus cuticle.

The goal of this study was to investigate the nature of Dopa distribution along the distal-proximal axis of the foot and thread and to explore how this correlates to the inorganic composition of the thread. We detected a gradient in the post-translational modification of tyrosine to Dopa along the length of the foot, and this gradient is exploited to fabricate an analogous gradient in the byssal thread. This is the first report of a spatial gradient of post-translational modification in a biomaterial. Perhaps related to the tendency of Dopa for complexation with metal ions, the Dopa gradient is closely coupled to similar trends in the distribution of Al and Fe.

## MATERIALS AND METHODS

**Mfp-1 Extraction**—Mussels used for this study were *M. galloprovincialis*. Excised mussel feet were frozen at  $-80^\circ\text{C}$  and depigmented by scraping the pigment off of the frozen tissue with a surgical blade. After depigmentation, each mussel foot was cut into seven equal sections as illustrated in Fig. 1A. Because each mussel foot has several glands in it including the phenol, accessory, collagen, and stem glands among others (3) and exhibits a gradient distribution of proteins along its length (25–28), feet selected for the experiments were almost the same size to minimize mixing of proteins from different parts of the foot. In the feet selected, section number 1 was usually the tip, and number 2 was usually the phenol gland or at least the majority of it. Mfp-1 was extracted based on previous studies (3). Briefly, same numbered sections were pooled and extracted with 1% perchloric acid. The samples were then microfuged at 14,000 rpm for 20 min, and the supernatants were saved. Duplicated samples with roughly the same amount of proteins were run on 10% acid-urea gel at 10 mA constant current and stained with Coomassie Blue R-250 for protein stain and nitro blue tetrazolium (NBT) for Dopa-containing protein stain, respectively.

**Mfp-1 Dopa Concentration Analysis**—Proteins (mainly mfp-1) extracted from the seven foot sections were loaded and run on 10% acid-urea gel followed by transferring to Immobilon membrane (Millipore) at 200 mA constant current for 1 h. After transfer, the membrane was stained with Coomassie Blue G-250, and the bands corresponding to mfp-1 were excised and hydrolyzed *in vacuo* at  $110^\circ\text{C}$  for 24 h in the presence of 6 M HCl and 10% phenol. Hydrolyzed samples were flash evaporated, resuspended and analyzed by a Beckman 6300 Autoanalyzer equipped with a dedicated HPLC according to Waite (29). Briefly, all amino acids including Dopa were separated by a Na-HPLC ion exchange column (Beckman Coulter number 338076) and detected by postcolumn ninhydrin derivatization. Elution signals were processed by HP ChemStation for LC.

**Thread Dopa Concentration Analysis**—Wild *M. galloprovincialis* threads were normalized and sectioned into six pieces as illustrated in

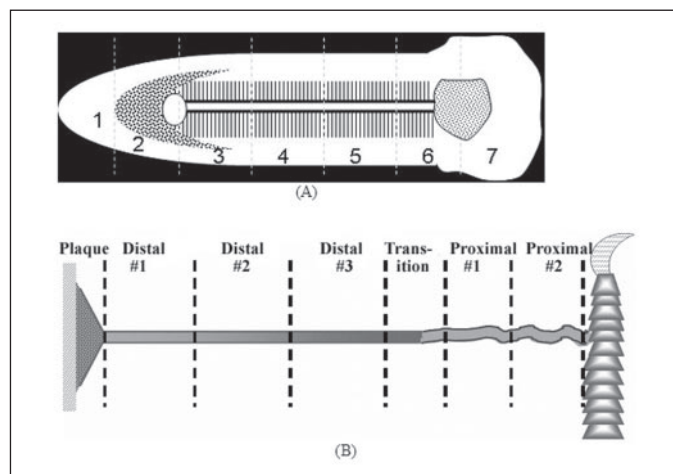


FIGURE 1. Schematic picture of a mussel foot (A) and thread (B), both serially segmented for analysis. A, section 1 is the tip of the foot and the distal end; it contained no detectable extracted proteins. Section 2 was mainly the phenol gland; section 3 had a small portion of the phenol gland, some accessory and collagen gland; sections 4 and 5 had both accessory and collagen gland; section 6 had accessory, collagen, and stem gland; and section 7 was mainly the stem gland. B, a schematic picture of one thread and the sections it was cut into. The distal portion of the thread was cut into three sections with equal length, and the proximal portion was cut into two sections with equal length. The overall length of the transition section was similar to or shorter than each proximal section.

Fig. 1B. Same numbered sections were pooled and hydrolyzed at  $158^\circ\text{C}$  *in vacuo* for 1 h. The hydrolysate was flash-evaporated and analyzed for amino acid composition as described above. Reported results were the average of three hydrolysates.

**Thread Metal Concentration Analysis**—To measure the concentration of the elements of interest in the different sections of the threads, normalized thread sections were first weighed and then hydrolyzed as above at  $158^\circ\text{C}$  *in vacuo* for 1 h, and the concentration of the elements were analyzed by inductively coupled plasma (ICP). The ICP used for this study was a TJA High Resolution IRIS model (Thermo Optic Inc., Franklin, MA). Standards used for analysis were purchased from High-Purity Standards, SC.

**Energy Dispersive Spectrometry (EDS) Line Scans**—To detect the distribution pattern of the elements of interest across a section of the thread, Q- $\text{H}_2\text{O}$ -washed threads were cut open under a dissecting microscope and mounted onto conductive carbon tape on scanning electron microscope posts with the cut surface facing up and lyophilized. The analysis was done on a FEI Co. XL30 environmental scanning electron microscope equipped with a Princeton Gamma Tech EDS with a PRISM IG intrinsic germanium detector for x-ray microanalysis. IMIX microanalysis software was used for x-ray acquisition, line profiles and analysis. Because of the nature of environmental scanning electron microscope, the tested samples did not need to be gold-coated.

**Thread Iron Accumulation Study**—Mussels maintained in circulating sea water tanks in the laboratory for at least 3 weeks after being collected from the wild were transferred to sea water adjusted to an equivalent iron concentration of 5 mM and maintained for 2 days with aeration. The high iron seawater was made by dissolving 5.406 g of  $\text{FeCl}_3 \cdot 6\text{H}_2\text{O}$  in deionized water then adding this solution to 4 liters of sea water with aeration for 1 h before introducing the mussels. The mussels did not produce any threads for the first 2 days, so the solution was diluted 10 times. Newly produced threads from each mussel were harvested after 48 h and washed thoroughly with Q- $\text{H}_2\text{O}$ . Treated threads were then dried and mounted on scanning electron microscope posts. The samples were sputter-coated with gold for 20 s using a Denton Vacuum DESK II coater (Moorestown, NJ) and examined with a Tescan

## Chemical Gradients in Byssal Thread

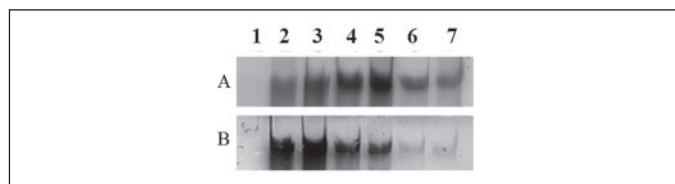


FIGURE 2. **Mfp-1** extracted from successive sections of a mussel foot and separated by acid-urea PAGE. *A* is stained for protein (CBR), and *B* is stained for Dopa using redox cycling (NBT). Gels were loaded with approximately the same amount of protein.

Vega TS 5130MM thermionic emission scanning electron microscope equipped with an IXRF energy dispersive spectrometer (Houston, TX).

### RESULTS

**Detecting Mfp-1 and Dopa by PAGE**—Previous work established that mfp-1s are selectively solubilized from acid-extracted mussel foot tissue by 1% perchloric acid. This convenient shortcut was exploited to extract mfp-1 from different sections of *M. galloprovincialis* foot. These extractions were run in parallel on acid-urea PAGE. One lot was stained for protein using Coomassie Blue R-250 (Fig. 2*A*) and the other for Dopa using a redox cycling stain (NBT) (Fig. 2*B*). We found that when loading roughly the same amount of protein in each lane based on the CBR stain intensity, there was a progressive decrease in NBT staining along the distal to proximal direction. Normally mfp-1 extracted from the section near the distal end stained most intensely with NBT. The gel results indicate that mfp-1 production by secretory cells along the foot appears to be coupled to an incrementally regulated post-translational modification of tyrosine to Dopa.

**Detecting Mfp-1 Dopa by Amino Acid Analysis**—To confirm the results suggested by gel CBR-NBT staining, microanalysis of protein transferred from the gel to Immobilon membranes (Millipore, MA) was performed. TABLE ONE shows that the composition of transferred bands corresponding to mfp-1 are consistent with the composition of bulk-purified mfp-1. Dopa/Tyr ratios in mfp-1 extracted from successive foot sections are seen in Fig. 3 to decrease from the tip to the base. Mfp-1 extracted from section #2 was mainly from the phenol gland vicinity (~3 mm from the tip) with a Dopa/Tyr of about 2.2, whereas the Dopa/Tyr in the mfp-1 extracted from the base of the foot was ~0.5. Therefore, Dopa is four times more abundant in mfp-1 from the distal portion as it is from the base of the mussel foot. We also calculated the combined contents of Dopa and Tyr, and this value remained essentially constant along the foot. This result supports the idea that the Dopa gradient in mfp-1 is established in the accessory gland cells before the protein is released into the ventral groove where the threads are molded.

**Detection of Dopa in Thread**—To determine whether the mfp-1 Dopa gradient in the foot is reflected in the thread, amino acid analysis of hydrolysates from different thread sections was performed, and the results are as shown in Fig. 4. The content of Tyr in mol % showed very little variation along the thread, whereas the levels of Dopa steadily decreased along the distal to proximal axis. Because the Tyr concentration did not change much along the thread, the ratio of the two followed the same trend as the change of Dopa. The results indicate that distal thread portions contain higher levels of Dopa than the proximal thread but also that Tyr-containing proteins besides mfp-1 are present in the thread.

**Metal Analysis by ICP**—Bulk concentrations of some metals and non-metallic elements of interest along the thread were analyzed by hydrolyzing thread sections (prepared in the same way as above) followed by ICP analysis. For better comparison, the concentrations of these elements in the plaque were also analyzed. As shown in Fig. 5, for each element tested, the concentration was frequently slightly higher in

|                  | Distal thread | Mfp-1 purified | Mefp-1 reported <sup>a</sup> | Mfp-1 cDNA |
|------------------|---------------|----------------|------------------------------|------------|
| Dihydroxyproline | 0.9           | 4.1            | 3                            |            |
| Hydroxyproline   | 8.2           | 10.7           | 10.2                         |            |
| Asx              | 7.2           | 3.8            | 2.2                          | 1.1        |
| Thr              | 2.8           | 10.9           | 11.7                         | 10.5       |
| Ser              | 6.1           | 8.4            | 10.2                         | 12.3       |
| Glx              | 4.4           | 2.3            | 0.9                          | 0.3        |
| Pro              | 4.9           | 6.7            | 8.1                          | 24.8       |
| Gly              | 28            | 3.3            | 3.2                          | 1.0        |
| Ala              | 16.8          | 7.5            | 8.1                          | 7.0        |
| Cys              | 0.2           | 0.5            | 0                            | 0          |
| Val              | 3.3           | 1.7            | 0.8                          | 0.5        |
| Met              | 0.03          |                | 0.1                          | 0.1        |
| Ile              | 1.4           | 1.0            | 0.8                          | 1.1        |
| Leu              | 2.1           | 1.1            | 1.1                          | 1.1        |
| Dopa             | 1.5           | 10.5           | 11.0                         |            |
| Tyr              | 2.1           | 7.2            | 7.0                          | 19.6       |
| Phe              | 1.1           | 0.4            | 0.1                          | 0.1        |
| His              | 1.0           | 0.6            | 0.7                          | 0.4        |
| Hydroxylysine    | 1.3           | 0.7            |                              |            |
| Lys              | 3.9           | 17.4           | 20.2                         | 19.6       |
| Arg              | 2.8           | 1.2            | 0.6                          | 0.5        |
| Total            | 100           | 100            | 100                          | 100        |

<sup>a</sup> Waite (11).

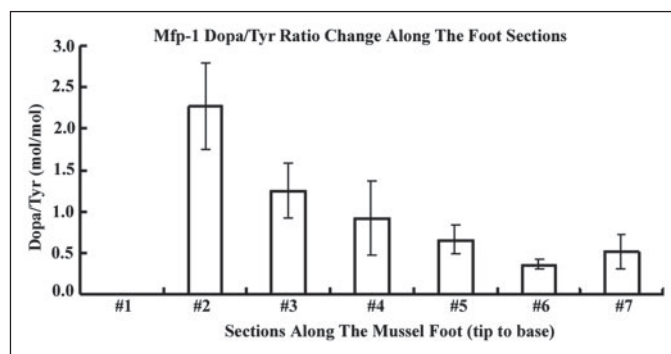


FIGURE 3. Changes in the molar ratio of Dopa/Tyr in mfp-1 extracted from different parts of mussel foot. #1–#7 denote sections as illustrated in Fig. 1.

the distal than the proximal region of the thread. There was very little variation among the sections that came from either the distal (Distal #1, #2, #3, and transition) or the proximal (proximal #1 and #2) region. Plaques always seemed to have the highest metal concentration in the samples tested.

**Elemental Analysis by EDS**—The distributions of the elements across the thread were examined by EDS. Fig. 6 shows a line scan through longitudinal cross-sections of the distal and proximal thread, respectively. The major elements found included sulfur, silicon, aluminum, and iron. Many of the elements were evenly distributed across the thread especially in proximal threads. However, some, notably sulfur, aluminum, and iron in distal thread sections, were not. Of these, aluminum, was localized to the outer thread periphery, whereas sulfur was broadly localized to the inner periphery. Iron was prominent and sharply localized to the outer cuticle region in the distal thread portions. However, EDS detected iron in only 50% of the threads sampled from

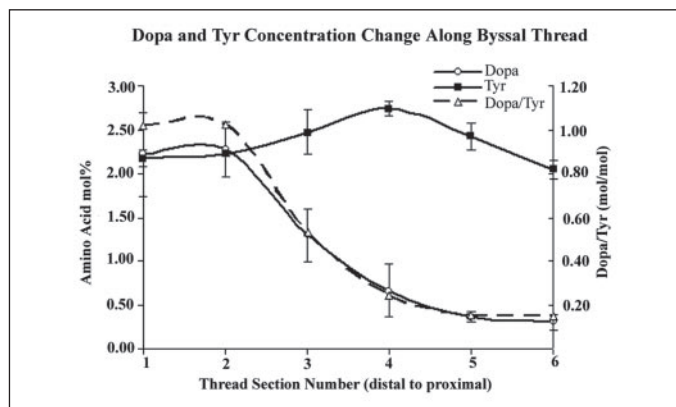


FIGURE 4. The change in molar percentage and molar ratio of Dopa and Tyr in successive thread sections (as in Fig. 1). Numbers in the abscissa represent thread sections. The dashed line is the molar ratio of Dopa/Tyr in each thread section and corresponds to the ordinate on the right side of the graph.

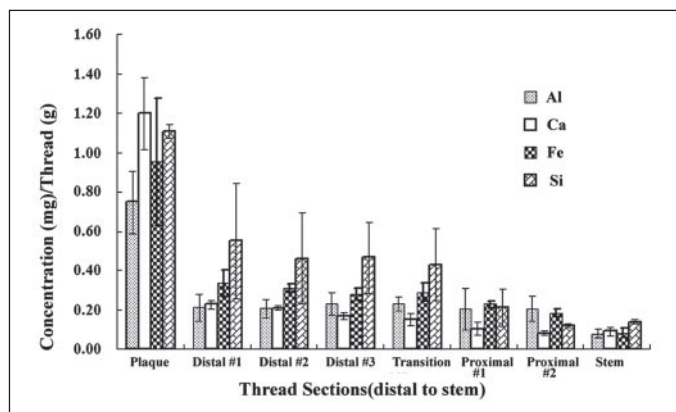


FIGURE 5. Total concentration of calcium (Ca), aluminum (Al), iron (Fe), and silicon (Si) as sampled from successive hydrolyzed thread segments. The concentration of each element was in units of mg/g of thread.

mussels maintained in tanks with circulating natural seawater for either short or long periods after their collection from the wild.

**Fe(III) Uptake Analysis**—The mussels first transferred into seawater supplemented with high iron (5 mM) were viable but did not produce any threads. Thread production started after the seawater was diluted 10 times (0.5 mM). When  $\text{FeCl}_3$  is added to seawater it reacts to form the insoluble  $\text{Fe}(\text{OH})_3$ . It was reported that the estimated concentration of the hydroxocomplex species of  $\text{Fe}^{3+}$  in seawater is  $\sim 0.01\text{--}1\text{ nM}$  (30, 31). Therefore, almost all of the iron we added was in particulate form. However, because we did not change anything besides the dilution of the iron supplement, we can assume that the iron particulates in the solution were  $\sim 10\%$  of the initial level. EDS line scan results as shown in Fig. 7 showed that iron was concentrated in the cuticle of the threads produced by mussels exposed to iron-supplemented seawater. On the other hand, threads made by mussels prior to the transfer from normal to iron-supplemented seawater did not show any enrichment of iron. Threads that were produced in normal seawater then incubated in iron-supplemented seawater without the attached mussels showed no sign of iron. Thus, iron incorporation into byssal threads is dependent on iron uptake by the live mussel and occurs only during the formation of a new thread.

## DISCUSSION

This is the first report of a spatial gradient involving a post-translational modification of any amino acid in a biological tissue. Previous

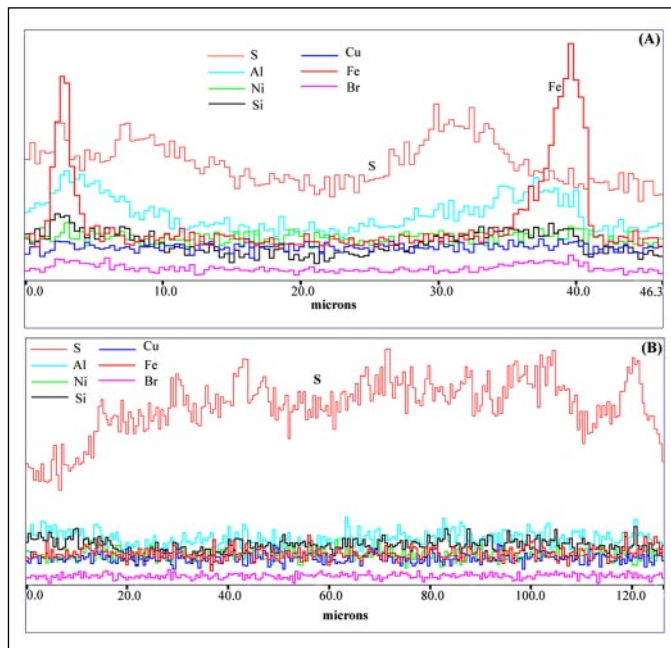


FIGURE 6. EDS line scan result of some elements across a cross-section of the thread. The y axis shows relative intensity. The arrow in the picture indicates the trajectory, which is the x axis of the scan. A, result on the distal portion of the thread. B, result on the proximal portion of the thread.

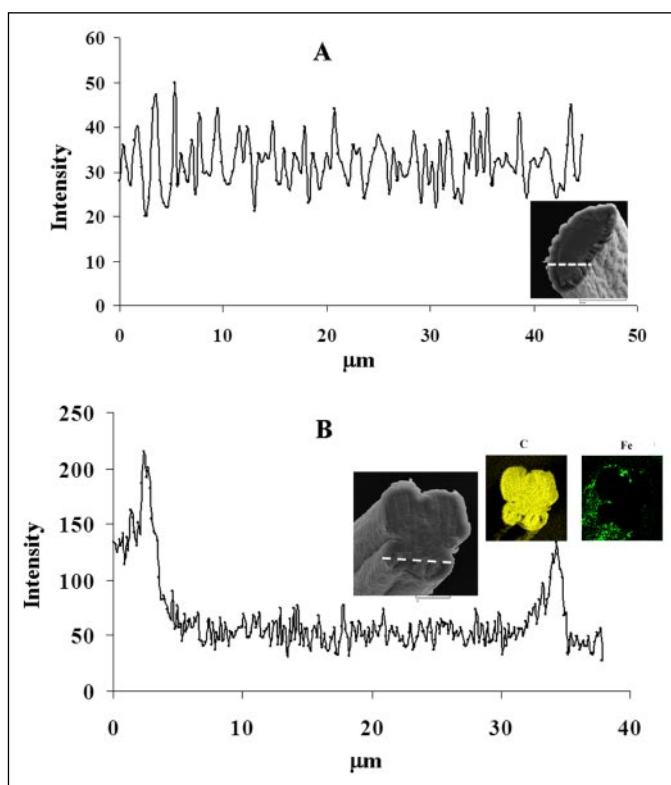


FIGURE 7. EDS line scan showing the iron distribution in the cross-section of distal thread. A, thread produced by mussel in untreated seawater was excised and incubated without mussel in iron-supplemented seawater for 2 days. B, thread produced by mussel in iron-supplemented seawater. Insets show the elemental mapping of carbon and iron by EDS.

studies of mussel byssus demonstrated protein gradients involving pre-Cols and matrix proteins in byssal threads (6, 28) as well as corresponding mRNA gradients in mussel foot (25, 26). From those studies, it was suggested that the gradients were established well before the proteins

## Chemical Gradients in Byssal Thread

were released into the ventral groove and processed into a thread (25). Successive foot extractions of mfp-1 make it clear that the Dopa gradient is also fabricated co- or post-translationally prior to secretion, but how the enzymes involved are regulated remains completely unknown.

It is not possible to extract mfp-1 from the thread and *in situ* localization is difficult because of rapid and extensive cross-linking (32, 33). Dopa is therefore commonly used as a surrogate for the protein. There are three known proteins that contribute Dopa residues to the distal thread composition. These are preCOL-D and -NG with Dopa levels of <1 mol % each, and mfp-1 with a high of 15 mol % (11). The core represents the greater portion (~85%) of thread volume and is dominated by the preCOLs in roughly equal parts, thus preCOLs could not contribute more than 0.5 mol % Dopa to thread composition. Mfp-1 is restricted to the cuticle, which is 4- $\mu$ m thick in a typical thread with 100- $\mu$ m diameter (5, 8). If mfp-1 is the only constituent in the cuticle, then the Dopa it contributes to the thread composition would be 2.1 mol %. In contrast, if mfp-1 fills only 0.5 of the volume of the cuticle then its Dopa contribution would be 1.05 mol %.

The Dopa concentration actually measured from the distal thread was 2.2 mol %. Therefore, after subtracting the preCOL contribution, the highest Dopa from mfp-1 would be 2.2 mol % - 0.68 mol % = 1.52 mol %, which is within the 1.05 mol % and 2.1 mol % boundaries defined above. Mfp-1 content of byssal threads can also be approached from another perspective. Purified mfp-1 contains ~6 mol % of a unique amino acid known as *trans* 2,3-, *cis* 3,4-, dihydroxyproline (13). This is a less attractive marker than Dopa for mfp-1, because it is more difficult to measure. If we are correct in assuming that mfp-1 is the only dihydroxyproline-containing protein in the thread and it is evenly distributed in the distal cuticle, the calculated dihydroxyproline mol % concentration in the distal thread would be 0.86 mol %. This number is very close to the mol % of dihydroxyproline (0.9 mol %) detected in the distal thread as shown in TABLE ONE and independently supports the assumptions made. The Dopa gradient in the thread is thus consistent with and results from a distal to proximal mfp-1 distribution that is uniform along the foot but with diminishing levels of Dopa.

Metal association with byssus is well known (18), and the byssus is often used as an environmental indicator for heavy metal pollution (34). ICP analysis of threads made in pristine seawater showed that the elements sampled, such as silicon, aluminum, and iron, all have higher concentrations in the distal than in the proximal portions. EDS line scans of threads were generally consistent with ICP data, with one notable anomaly. Iron was detected by EDS in only 50% of the threads, although ICP analysis consistently indicated moderate amounts. This is not necessarily contradictory given that ICP analysis requires many threads, whereas EDS samples a single thread at a time. When iron was detected by EDS, it was sharply localized to the cuticle of the thread. It is not known whether the threads were equally functional with and without iron, but their appearance was the same.

Our studies show conclusively that exposure of mussels with iron-deficient threads to iron-supplemented seawater resulted in enhanced iron deposition in the cuticle of all the threads tested. This suggests that iron deposition in byssal threads is based not only on the availability of iron, but the availability of iron in any form. Because the solubility of iron is only 0.01–1 nM in seawater, even supplements of soluble iron will be transformed to colloidal iron hydroxide with a solubility product ( $K_{sp}$ ) of only  $10^{-39}$ . This would require a very aggressive iron recovery strategy in the gut and/or gills of the mussel. Because catechols like Dopa have very high binding affinities for Fe(III) ( $\log K_s$  of 45) and are concentrated in the cuticle, it is very probable that at least some of the

Dopa acts as a mordant for the iron *in situ* and that this association serves some biological function. The results suggest that thread formation in *Mytilus* may be more adaptable than previously thought. When particulate iron is abundant, as would be expected in a wave-swept seashore habitat, the thread cuticle becomes ironclad; when iron is limiting such as in the laboratory aquarium, a cuticle is made without iron.

Threads appear to be fully functional in uniaxial tension with or without iron, and Dopa seems equally recoverable, at least in short term experiments, from iron-deficient and iron-enhanced threads following acid hydrolysis. We suspect that ironcladding may in some way improve the wear resistance of the exposed distal portion of the byssus, and a mechanical analysis is underway.

---

*Acknowledgments*—We thank Dr. Jose Saleta at Donald Bren School of Environmental Science and Management at UC Santa Barbara for acquiring the EDS spectra, James Weaver for helping with SEM and imaging, Dr. Joe Doyle at Material Research Laboratory at UC Santa Barbara for helping with ICP, Xin Zhang for helping with protein purification and amino acid analysis, and Niels Holten-Andersen and Scott Jewhurst for valuable discussion.

---

## REFERENCES

1. Waite, J. H., Vaccaro, E., Sun, C., and Lucas, J. M. (2002) *Philos. Trans. R. Soc. Lond. B Biol. Sci.* **357**, 143–153
2. Suresh, S. (2001) *Science* **292**, 2447–2451
3. Waite, J. H. (1992) in *Biopolymers* (Case, S. T., ed) Vol. 19, pp. 27–54, Springer-Verlag, Berlin
4. Vitellaro-Zucarello, L. (1981) *Tissue Cell* **13**, 701–713
5. Holten-Andersen, N., Slack, N., Zok, F., and Waite, J. H. (2005) in *Mechanical Properties of Bioinspired and Biological Materials* (Viney, C., Katti, K., Ulm, F., and Hellmich, C., eds) pp. 155–160, Materials Research Society, Warrendale, PA
6. Qin, X. X., and Waite, J. H. (1995) *J. Exp. Biol.* **198**, 633–644
7. Hassenkam, T., Gutschmann, T., Hansma, P., Sagert, J., and Waite, J. H. (2004) *Biomacromolecules* **5**, 1351–1355
8. Benedict, C. V., and Waite, J. H. (1986) *J. Morphol.* **189**, 171–181
9. Bell, E. C., and Gosline, J. M. (1996) *J. Exp. Biol.* **199**, 1005–1017
10. Vaccaro, E., and Waite, J. H. (2001) *Biomacromolecules* **2**, 906–911
11. Waite, J. H. (1983) *J. Biol. Chem.* **258**, 2911–2915
12. Waite, J. H., Housley, T. J., and Tanzer, M. L. (1985) *Biochemistry* **24**, 5010–5014
13. Taylor, S. W., Luther, G. W., and Waite, J. H. (1994) *Inorg. Chem.* **33**, 5819–5824
14. Inoue, K., and Odo, S. (1994) *J. Biol. Bull.* **186**, 349–355
15. Dalsin, J. L., Hu, B. H., Lee, B. P., and Messersmith, P. B. (2003) *J. Am. Chem. Soc.* **125**, 4253–4258
16. Dalsin, J. L., Lin, L., Tosatti, S., Voros, J., Textor, M., and Messersmith, P. B. (2005) *Langmuir* **21**, 640–646
17. Waite, J. H. (1990) *Int. J. Biol. Macromol.* **12**, 139–144
18. Taylor, S. W., Chase, D. B., Emptage, M. H., Nelson, M. J., and Waite, J. H. (1996) *Inorg. Chem.* **35**, 7572–7577
19. Coombs, T. L., and Keller, P. J. (1981) *Aquat. Toxicol.* **1**, 291–300
20. Tateda, Y., and Koyanagi, T. (1986) *Bull. Jpn. Soc. Sci. Fish.* **52**, 2019–2026
21. Coulon, J., Truchet, M., and Martoja, R. (1987) *Ann. Inst. Oceanogr., Paris*, **63**, 89–100
22. George S. G., Pirie B. J. S., and Coombs T. L. (1976) *J. Exp. Mar. Biol. Ecol.* **23**, 71–84
23. Frank, B. P., and Belfort, G. (2002) *Biotechnol. Prog.* **18**, 580–586
24. Sever, M. J., Weisser, J. T., Monahan, J., Srinivasan, S., and Wilker, J. J. (2004) *J. Angew. Chem. Int. Ed.* **43**, 448–450
25. Qin, X. X., Waite, J. H. (1998) *Proc. Natl. Acad. Sci. U. S. A.* **95**, 10517–10522
26. Coyne, K. J., and Waite, J. H. (2002) *J. Exp. Biol.* **203**, 1425–1431
27. Waite, J. H., Qin, X. X., and Coyne, K. J. (1998) *Matrix Biol.* **17**, 93–106
28. Sun, C., Lucas, J. M., and Waite, J. H. (2002) *Biomacromolecules* **3**, 1240–1248
29. Waite, J. H. (1991) *Anal. Biochem.* **192**, 429–433
30. Kuma K., Katsumoto, A., Kawakami H., Takatori, F., and Matsunaga, K. (1998) *Deep Sea Res. Part I*, **45**, 91–113
31. Liu, X., and Millero, F. J. (2002) *Mar. Chem.* **77**, 43–54
32. Anderson, K. E., and Waite, J. H. (2000) *J. Exp. Biol.* **203**, 3065–3076
33. Robinson, M.W., Colhoun, L. M., Fairweather, I., Brennan, G. P., and Waite, J. H. (2001) *Parasitol.* **123**, 509–518
34. Koide, M., Lee, D. S., and Goldberg, E. D. (1982) *Estuarine, Coastal and Shelf Science* **15**, 679–695